Escherichia coli Ribosomal 5S RNA–Protein L25 Nucleoprotein Complex: Effects of RNA Binding on the Protein Structure and the Nature of the Interaction†

Matthew J. Kime and Peter B. Moore*

ABSTRACT: The complexes of three variants of *Escherichia coli* 5S RNA with ribosomal protein L25 have been studied by high-field proton nuclear magnetic resonance. A spectroscopic method is demonstrated to help distinguish the macromolecular sources of proton resonances in nucleoprotein complexes. The effects of L25 binding on the three RNAs tested were small; the presence of the L25 did not strongly influence the conformation of the RNA. The interaction of L25 with 5S RNA produced modest, but distinctive, alterations in the protein spectrum, in both the aromatic region and the upfield spectrum. As judged by these changes, the mechanism of binding was the same in all three cases. The changes seen in the spectrum of L25 indicate that its conformation is not altered in a major way upon RNA binding. Arginine residues appear to be involved in the binding mechanism. Intercalation of L25 aromatic residues with RNA bases does not appear to play a role in the interaction.

Many phenomena in molecular biology are based on sequence-specific interactions between proteins and nucleic acids. Nuclear magnetic resonance (NMR)[1] spectroscopy is a powerful tool for studying macromolecular conformation in solution and has great potential for examining interacting systems of this kind. The relaxation characteristics of macromolecules, however, mean the technique is best applied to relatively small nucleoproteins. The complex which forms between *Escherichia coli* ribosomal 5S RNA and protein L25 has proven to be a suitable system. A recent NMR study of the 5S RNA–L25 complex in ^1H_2O solution has given some insights into the effects of protein binding upon the structure of 5S RNA (Kime & Moore, 1983a). Here, we address the related topics of the effects of RNA binding upon the conformation of protein L25 and the nature of the protein–nucleic acid interaction.

Three variants of 5S RNA complexed with L25 have been studied. Intact 5S RNA can exist in two different conformers at neutral pH, both of which are native, or "A form", 5S RNA by normal criteria. One form, the H form, is seen in the presence of Mg^{2+}. The second conformer, the L form, is seen in the absence of Mg^{2+}. Both forms bind L25 (Kime & Moore, 1982). The L25 complexes with both H- and L-form 5S RNA are examined below. The third complex studied involves a nucleolytic fragment of 5S RNA. Limited digestion of 5S RNA leads to the formation of a complex of strands of the parent molecule consisting of bases 1–11, 69–87, and 89–120 in high yield. This fragment of 5S RNA also binds L25 (Douthwaite et al., 1979; Kime & Moore, 1983a–c). Data on its effect on the L25 conformation are also presented here.

A major difficulty in nucleoprotein NMR spectroscopy is distinguishing those resonances which are due to protein protons from those due to nucleic acid protons. Unless such distinctions can be made, even qualitative comparison of the structures of the isolated components of a complex with the structures they assume in the complex is impossible. Further, the sorting of resonances as to macromolecular type is a necessary first step toward complete assignment of the complex spectrum.

The reason classifying resonances can be difficult is that resonances from free protein and nucleic acid overlap. Furthermore, one lacks a priori knowledge of the perturbations occurring as a consequence of complex formation which means that knowledge of the spectra of the uncomplexed species is not a sure guide to understanding the spectrum of the complex. Moreover, "hybrid" resonances, those which represent protons involved in linking the protein to the nucleic acid (e.g., quaternary hydrogen bonds), may be generated.

Figure 1 [drawn using the data given in Campbell & Dobson (1979) with minor changes] illustrates potential resonance overlaps in nucleoprotein proton NMR spectra. The RNA base imino protons, which resonate in the far-downfield region, are probably the most tractable set of resonances to study from this viewpoint, but the information to be gained from this class of protons is mainly related to nucleic acid structure. We wished to study the protein in the complex. Most of the experiments reported here were performed in ^2H_2O solution. This simplified the proton NMR spectra by permitting us to observe nonexchangeable protons exclusively. (All resonances with an NH in the description in Figure 1 are exchangeable and are absent in spectra of samples dissolved in ^2H_2O.)

Isotopic enrichment schemes may be devised to aid assignment of resonances as to macromolecular species, but such methods are often tedious and expensive. We demonstrate below a purely spectroscopic method which helps distinguish the macromolecular sources of proton resonances in nucleoprotein complexes. Selective irradiation at the frequency at which many RNA ribose protons resonate (ca. 4.2 ppm) saturates all the ribose protons, and efficient local cross-relaxation (negative NOEs) markedly reduces the intensity of the RNA aromatic base protons. Difference spectra accumulated with on- and off-resonance decoupling on nucleoprotein complex samples are characterized by aromatic regions (9.0–6.0 ppm), where overlap is ordinarily most severe, which

† From the Department of Chemistry, Yale University, New Haven, Connecticut 06511. *Received September 26, 1983.* This research was supported by grants from the National Institutes of Health (AI-09167 and GM-32206). NMR spectroscopy was done at the Northeast Regional NMR Facility which is supported by the National Science Foundation (Grant CHE-7916210). M.J.K. is a NATO/British Science and Engineering Research Council postdoctoral fellow.

[1] Abbreviations: NMR, nuclear magnetic resonance; Tris, tris(hydroxymethyl)aminomethane; NOE, nuclear Overhauser effect; TMV, tobacco mosaic virus.

0006-2960/84/0423-1688$01.50/0

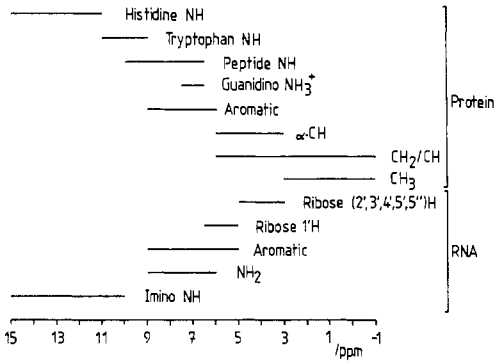

FIGURE 1: Chemical-shift ranges (in ppm) of isolated protein and ribonucleic acid proton resonances [drawn with data from Campbell & Dobson (1979) with minor modifications]. The protons labeled with an "NH" in the description are exchangeable and should not be detected in samples in ^2H_2O buffer.

are dominated by the protein contribution.

Several conclusions emerge from the data. First, the effect of the binding of L25 to any of the three RNAs tested is small; its presence does not strongly influence the conformation of its RNA ligand. Second, the interaction of L25 with RNA leads to modest, but distinctive, alterations both in the protein aromatic spectrum and in its upfield spectrum (from 4.0 to −1.0 ppm). These changes are seen when L25 binds to each of three RNA ligands tested, indicating that the mechanism of binding is the same in all three cases. Third, the changes seen in the spectrum of L25 suggest that its conformation is not altered in a major way upon RNA binding and further suggest an involvement of arginine residues in the binding mechanism. The modest alterations seen in the aromatic regions of spectra both of L25 and of its RNA ligands upon binding rule out the possibility that intercalation of L25 aromatic residues with RNA bases might play a role in this interaction.

Materials and Methods

L25. Ribosomal protein L25 was prepared as described previously (Kime et al., 1981; Kime & Moore, 1982).

Ribosomal 5S RNA. This was purified from 70S ribosomes or 50S subunits (*E. coli* MRE 600) as described elsewhere (Kime & Moore, 1982). For some experiments done on 5S fragment, the starting 5S RNA was purified from whole-cell, low molecular weight RNA (*E. coli* B) purchased from Plenum Scientific Research (Hackensack, NJ). 5S RNA was purified from this mixture by chromatography on Sephacryl S200 in 0.15 M NaCl, 1% methanol, and 0.1 M sodium acetate (pH 5.0).

5S RNA Fragment. The preparation of fragment has been described elsewhere (Kime & Moore, 1983b). 5S RNA at 1 mg/mL was exposed to 10 μg/mL RNase A at 0 °C for 45 min at pH 7.8. Following digestion, RNase was removed by phenol extraction and the fragment purified by chromatography on Sephadex G-75.

L25–5S RNA Complexes. Prior to complex formation, the isolated macromolecules, L25 and 5S RNA, were suspended at relatively dilute concentrations (typically 0.1 mM) in the buffers to be used for subsequent NMR spectroscopy (with the exceptions that they were in ^1H_2O and no chemical-shift reference was added). Complexes were formed by adding L25 to the aqueous RNA. The resulting mixtures were concentrated by ultrafiltration using Amicon YM-5 filters to obtain samples with concentrations of approximately 1.0 mM.

NMR Samples. The macromolecular samples in NMR buffer (but in ^1H_2O solvent) were concentrated, if necessary, by ultrafiltration to approximately 0.5 mL and then dialyzed repetitively (from 4 to 6 times) against about 5-mL aliquots of the NMR buffer (described in the figure legends) in 99.8% ^2H_2O.

NMR Spectroscopy. All spectra were accumulated on a Bruker WM-500 NMR spectrometer operating in the Fourier transform mode. Samples were held at 302 K for data acquisition. Dioxane was introduced as a chemical-shift standard, and its single proton NMR resonance was assumed to have a chemical shift of 3.741 ppm relative to the upfield methyl resonance of 3-(trimethylsilyl)propanesulfonic acid.

Spectra displayed in the text, except the one shown in Figure 6a, were acquired by block averaging; i.e., sets of spectra were collected and stored consecutively on each sample, exponential multiplication was applied where suitable, and the individual spectra in each set were Fourier transformed and phase corrected before addition to create the spectra as shown.

Data were collected on each sample by using three different sets of acquisition parameters in succession. (a) A 16K block size spectrum was accumulated with a 6.4-s pulse cycle time by using 90° pulses and 240 transients. (b) Several 8K block size spectra were collected with a 0.7-s pulse cycle time by using 50° pulses to total 2400 transients. (c) Several 8K block size spectra were acquired with a 1.2-s pulse cycle time by using 50° pulses to total 2400 transients, and a 0.5-s selective presaturation pulse was applied at about 4.2 ppm prior to acquisition of each transient. The presaturation pulse power was chosen after a series of control experiments on the L25–5S complex specimen of a sample set. As high a power as possible which did not detectably affect the intensity due to protein in the resulting spectra was used.

This data collection regime was adopted for several reasons: (1) the 6.4-s pulse cycle time spectra were found to display a major base-line distortion at the receiver gain settings available. The samples retained a significant HOD concentration, and a dynamic range problem (which was more severe than expected with the 16-bit digitizer used) resulted when the water protons had sufficient time to relax fully, or nearly so. Such 6.4-s pulse cycle times would have ensured effectively complete relaxation of macromolecular protons, and the resulting spectra would then have represented absolute intensity information. (2) Relatively rapid accumulation of spectra, with adequate signal to noise for differencing, of the low concentration samples studied could be achieved only by short pulse cycle times. The data produced could then be compared with the (noisier and distorted) 6.4-s pulse cycle time control spectrum on the same sample to judge if, and how, intensities had been modified by allowing insufficient relaxation time. Such comparisons indicate that the relative intensities of spectra of intact 5S RNA containing samples (e.g., 5S RNA or 5S RNA–L25 complex samples) are not significantly affected by increasing the pulse cycle time above 0.7 s. Samples containing free L25 or free 5S RNA fragment, however, did have significantly increased intensities (not necessarily uniformly across the spectrum because the one correlation time description of a macromolecule is only an approximation) when longer pulse cycle times were employed.

Difference Spectra. The qualitative relaxation results described in the previous section require that the methods used for generating difference spectra be described. It is pointed out that a spectrum of the relatively small molecule, protein L25, is used on only one occasion to create a difference spectrum (Figure 2e), and to generate this difference, the protein spectrum intensity was anomalously weighted, and a line broadening was applied to match both the intensity and

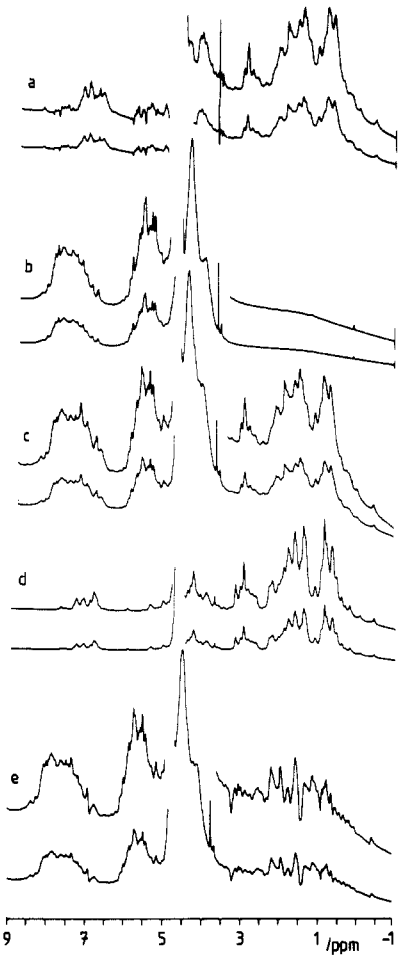

FIGURE 2: Spectra of the intact 5S RNA–L25 complex and its macromolecular components in 2 mM $MgCl_2$, 10 mM [$^2H_{11}$]Tris-^{2}HCl (Merck Sharp & Dohme), 5 mM [$^2H_6$]ethanol, 0.1 M KCl, and ^2H_2O, pH 7.8, buffer. (b) 0.66 mM 5S RNA; (c) 0.76 mM 5S RNA–L25 complex; (d) 1.3 mM L25; (a) spectrum c minus spectrum b; (e) spectrum c minus spectrum d. The insets have double vertical display scales to make comparisons between spectra easier.

the average line width of its spectrum to those of the complex spectrum with which it was being compared. Otherwise, spectral differences were computed by direct subtraction of spectra accumulated with a similar number of scans on samples with roughly matching concentrations. When subtractions were performed which took into account the exact concentrations of the samples used, and weighted the spectra appropriately, the differences obtained were barely distinguishable from those presented: the quality of the differences was little affected by the weighting factors used within the range of concentration differences in the sample sets used in this work (equality ±30%). Perhaps most significantly one full set of 6.4-s pulse cycle time spectra was accumulated with a good signal to noise ratio on the H-form 5S RNA–L25 complex set of samples, and the difference spectra produced differ in no material respect from the differences presented below (except that there is a pronounced base-line distortion).

Practical Notes. It was found by chance that the solubility of protein L25 increases in the presence of a low concentration of ethanol, as judged by visual examination of the samples. Many samples containing L25 were made 0.1% in [$^2H_6$]ethanol (Stohler Isotopes). This had no detectable effect on the L25 spectrum.

It is our impression that the addition of Mg^{2+} (by dialysis) at 2 mM or greater affects the free protein L25 spectrum. These effects include the appearance of a broad resonance at about −0.3 ppm and the broadening of the histidine resonance at about 7.6 ppm as well as other intermediate exchange phenomena.

Some broad downfield resonances are visible in some spectra of samples which had been dialyzed against many changes of ^2H_2O buffer.

Results

5S RNA–L25 Nucleoprotein Complex in Mg^{2+}–^2H_2O. Figure 2 shows spectra of 5S RNA (b) and a stoichiometric 5S RNA–L25 complex (c) and the difference spectrum (a) of spectrum c minus spectrum b. A detailed interpretation of the spectra is impeded by the overlaps of relatively broad macromolecular resonances. This figure demonstrates the approximate distributions of proton intensities in the free macromolecule and complex spectra. The spectral region with most intensity in these spectra is the envelope of RNA ribose proton resonances. Figure 2 has inserts with double vertical gain for other spectral regions. The 5S RNA spectrum is confined within the chemical-shift range 8.5–4.0 ppm in agreement with the Figure 1 data for ribonucleic acids in ^2H_2O solution. The 5S RNA–L25 complex spectrum (c) has relatively small differences compared to spectrum b within this chemical-shift range (8.4–4.0 ppm) but has additional resonances which resemble free protein resonances in the chemical-shift range from 4.0 to −1.0 ppm. The difference spectrum (a) must contain the spectrum of RNA-bound L25 and the difference between the spectra of free and protein-bound 5S RNA. (New intensity representing "hybrid" resonances of protons bridging the two species in the complex is not expected to be detected in a complex sample equilibrated with ^2H_2O over long periods.)

Figure 2 also displays the spectra of L25 (d) and the stoichiometric 5S RNA–L25 complex (c) and the difference spectrum (e) for spectrum c minus spectrum d. The protein spectrum (d) is typical of that of a small globular protein and is essentially the same as that published earlier (Kime et al., 1981). Attention is drawn to the following two spectral regions: (i) the upfield-shifted methyl region (0.8–0.5 ppm) and (ii) the aromatic region (8.0–6.0 ppm). The upfield-shifted methyl region of a protein often has resolved resonances representing single methyl groups. These methyls have large secondary chemical shifts because they are close to ring-current shifting centers (in a protein these are usually the aromatic side chains). Resolution is significant because it may permit assignment of the resonances to specific residues or, failing that, to particular residue types. The aromatic region of a protein spectrum is similarly significant; there are usually few aromatic residues in proteins, and the resonances of aromatic protons present are often well enough resolved, so again assignment may be possible [see Campbell & Dobson (1979) for further information on protein spectral assignments]. The difference spectrum (e) must contain the spectrum of protein-bound 5S RNA and the difference between free and RNA-bound L25 spectra. Figure 3 shows the downfield of water region at higher vertical gain of the L25 spectrum (a) and the difference spectrum from Figure 2a (b). Several conclusions can be drawn from these spectra. (i) In both difference spectra (Figure 2a,e), the effects of protein binding on the 5S RNA moiety are difficult to observe spectroscopically; they are small. (ii) In the difference spectrum of Figure 3b, it is clear that the aromatic spectrum of the bound protein (8.0–6.0 ppm) displays many features in common with the aromatic spectrum of the free protein spectrum (see Figure 3a), but there are some effects due to the binding of RNA. (iii) In the difference spectrum of Figure 2e, there are sub-

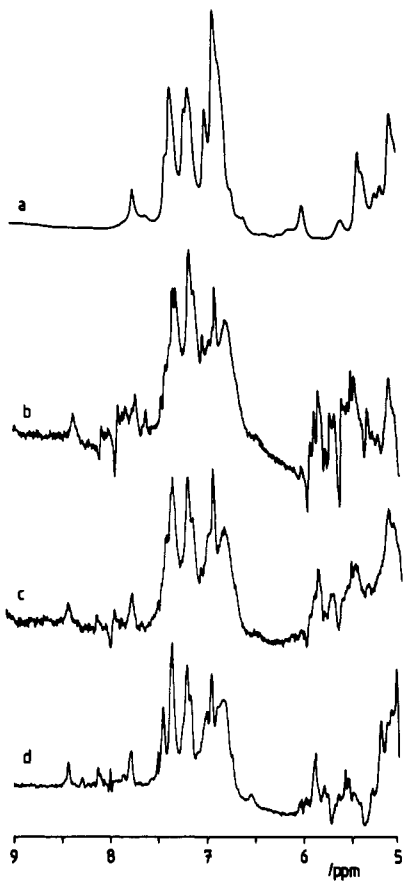

FIGURE 3: Comparison of the downfield of water regions of a spectrum of isolated protein L25 (a) (the sample is that used for Figure 2d) with difference spectral representations of the bound L25 [(b) as in Figure 2a, (c) the difference between spectra of the presaturated H-form 5S RNA–L25 complex and presaturated H-form 5S RNA using the samples described in Figure 2 and (d) as in Figure 7c].

stantial intensity changes upfield of 4.0 ppm. Particularly notable is the disappearance of most of the protein intensity at 3.2 ppm upon complex formation. (iv) As far as may be determined from the spectra presented, binding of protein to 5S RNA does not significantly increase the line widths of the 5S RNA resonances, but protein resonances are significantly broader in the complex spectrum than in the free protein spectrum. The incremental increase in the molecular size of RNA by binding L25 (an addition of a protein of molecular weight ca. 11 000 to an RNA of molecular weight ca. 39 000) is far less significant than the incremental increase in size of L25 by binding 5S RNA.

In the experiments described, satisfactory difference spectra were obtained showing the RNA-bound L25 aromatic region (Figure 2a), but these difference spectra necessarily include contributions due to alterations in the RNA aromatic spectrum upon protein binding. These RNA contributions make it difficult to interpret the difference spectra in regions of possible overlap. Therefore, means were sought for selectively suppressing the RNA contributions to the spectrum of the complex with the intention of obtaining a complex minus RNA difference spectrum which was as close as possible to a pure bound protein spectrum.

Presaturation of Ribose Proton Contributions to the 5S RNA Spectrum. The method used for RNA suppression was based on the chance observation that suppression of residual ^1H_2O signals in RNA samples dissolved in ^2H_2O by selective, gated irradiation at the water resonance frequency (Campbell et al., 1974) strongly suppressed the entire spectrum. Further investigation of the effects of irradiation power levels and

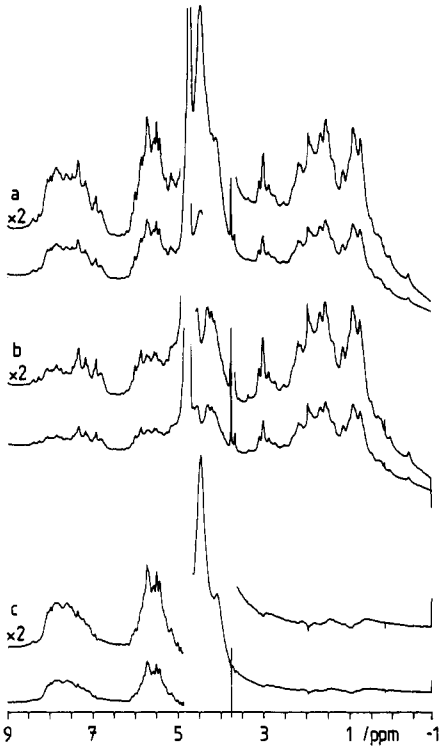

FIGURE 4: Demonstration of the effects of selective irradiation at 4.2 ppm on H-form 5S RNA–L25 complex spectra. The sample is that described in Figure 2. (a) The spectrum without irradiation; (b) the spectrum using the presaturation pulse sequence; (c) spectrum a minus spectrum b.

frequency on suppression revealed that the RNA spectrum was most effectively reduced by selective irradiation of the ribose proton peak at 4.2 ppm, not the ^1H_2O peak at 4.7 ppm. Figure 4 illustrates the effect on spectra of the 5S RNA–L25 complex. Figure 4a shows spectra of a stoichiometric 5S RNA–L25 complex (a) and of the same sample with presaturation at ca. 4.2 ppm (b) and the difference spectrum (c) for spectrum a minus spectrum b. RNA contributions in the aromatic region are obviously reduced in the spectrum b accumulated by using presaturation. The difference spectrum (c) clearly resembles an RNA spectrum. Similar experiments performed on 5S RNA in the absence of protein demonstrated that presaturation reduces RNA intensities in the aromatic region (8.2–6.8 ppm) to about one-fourth of the intensity otherwise observed. In the region from 6.2 to 5.0 ppm, presaturation reduces the intensity to about one-third its normal level.

Similar reductions have been reported in the intensities of resonances of both exchangeable and nonexchangeable protons in $tRNA^{Phe}$ upon presaturation of solvent ^1H_2O protons at about 4.7 ppm (Johnston & Redfield, 1978). This reduction was observed in 95% or 40% ^1H_2O. The suggestion was made that the effect on nonexchangeable proton intensities includes an important component of magnetic dipole coupling between these protons and ^1H_2O. The fact demonstrated here that presaturation at 4.2 ppm in ^2H_2O, which should mediate such interactions very inefficiently, also reduces the intensity of nonexchangeable proton resonances very effectively suggests an alternative explanation for the observations of Johnston & Redfield (1978), namely, that the presaturation irradiation at 4.7 ppm was not sufficiently selective to avoid saturating some RNA protons directly. Once these RNA protons are saturated, as is clear from the experiments with irradiation at 4.2 ppm, local intramolecular cross-relaxation ensures reduction of the other carbon (nonexchangeable) proton resonance intensities.

There is some differentiation in the efficiency with which intensity is removed in the RNA aromatic region by these negative NOE effects; not all features are uniformly suppressed. This is taken to indicate that the protons with less significantly perturbed resonances are aromatic base protons at a greater than average distance from ribose protons. (It may be noted that subsequent attempts to suppress the imino proton resonances of RNA involved in nucleoprotein complexes in ^1H_2O solution by presaturation at 4.2 ppm have not been successful. In addition to the experimental difficulty of irradiating at a frequency close to that of ^1H_2O without reducing the efficiency of ^1H_2O suppression by tailored-pulse methods, the intensities of the imino proton resonances do not appear to be measurably affected.)

The difference spectrum in Figure 4c should give a good approximation of the spectrum of L25-bound 5S RNA without any contributions due to L25, but including whatever NOE differentiation effects may occur in the complex. Comparison of the aromatic (8.2–6.8 ppm) and the ribose 1′H and pyrimidine C5H (6.2–5.0 ppm) regions of Figure 4c and the same regions of a difference (normal minus ribose presaturated) spectrum of free 5S RNA (data not shown), obtained under similar conditions, confirms that it is difficult to discern any spectroscopic differences between bound and free 5S RNA.

In Figure 4c, there is some intensity seen in the region upfield of 4.0 ppm. This could be bad differencing, but it could equally be the manifestation of spin diffusion in the L25 moiety of the 5S fragment complex as detected in similar experiments in ^1H_2O at low temperatures (Kime & Moore, 1983a). Here the spin diffusion could be produced by presaturation of the protein intensity at ca. 4.2 ppm or by the irradiation of the ribose intensity at that chemical shift (or both). It is not possible to distinguish the effects with the data at hand. Under identical presaturation conditions, spin diffusion effects were not observed when a free protein L25 sample was irradiated at 4.2 ppm.

Presaturation at 4.2 ppm in 5S RNA–L25 Complex Spectra. Figure 4 and the preceding section have used presaturation at 4.2 ppm in 5S RNA–L25 complex spectra to reduce the RNA contribution to the complex spectrum and to examine the form of the protein-bound RNA. In the aromatic region of the spectrum acquired using presaturation (Figure 4b), the bound L25 intensity is the dominant feature.

Spectra were recorded of 5S RNA by using ribose presaturation and also of the stoichiometric 5S RNA–L25 complex by using ribose presaturation. A difference spectrum (complex minus free RNA) was computed. Figure 5b shows the difference spectrum. Figure 5a shows a spectrum of free protein L25 in the presence of magnesium ions for comparison. The expanded downfield of water region of the difference spectrum is presented in Figure 3c. This difference spectrum is superior to the previous difference spectrum showing bound L25 (in Figures 2a and 3b) because, although it contains some spectral information due to perturbation of the RNA, most of the RNA intensity was suppressed by the presaturation before differencing: it is almost a pure bound L25 spectrum.

5S RNA Fragment in Mg^{2+}–^2H_2O. A series of experiments similar to those discussed above were carried out by using the ribonuclease A resistant fragment derived from 5S RNA as the RNA moiety rather than intact 5S RNA. Figure 6 shows the spectra of intact 5S RNA (a) and of the uncomplexed 5S RNA fragment (b). The small size of the fragment relative to intact 5S RNA makes for more rapid tumbling of the fragment molecules in solution, longer relaxation times, and better resolved spectra (narrower lines). A reduction in the number of protons per molecule (to about half of those in intact 5S RNA) also helps by simplifying the spectrum.

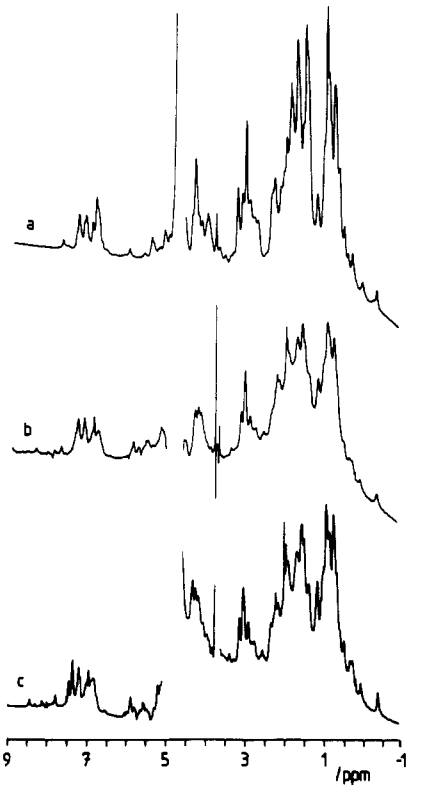

FIGURE 5: Comparison of the spectra of isolated protein L25 (a) using the sample described in Figure 2d with difference spectral representations of the bound L25 [(b) the difference between spectra of the presaturated H-form 5S RNA–L25 complex and presaturated H-form 5S RNA using the samples described in Figure 2 and (c) as in Figure 7c].

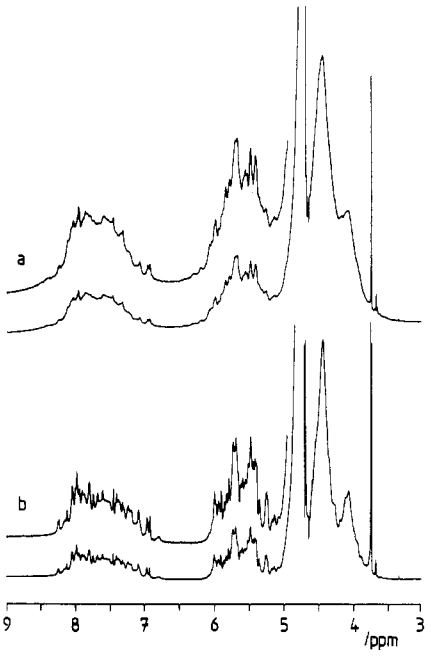

FIGURE 6: Comparison of the spectrum of (a) 0.55 mM H-form 5S RNA in 2 mM $MgCl_2$, 10 mM [$^2H_{11}$]Tris-^{2}HCl, 0.1 M KCl, and ^2H_2O, pH 7.6 at 300 K (1000 transients with a 1.5-s pulse cycle time), with that of (b) 0.63 mM *E. coli* B 5S RNA fragment in 3 mM $MgCl_2$, 10 mM [$^2H_{11}$]Tris-^{2}HCl, 0.1 M KCl, and ^2H_2O, pH 7.5.

Spectra were acquired of 5S RNA fragment and of a stoichiometric 5S fragment–L25 complex. The difference spectrum was computed (data not shown). The fragment

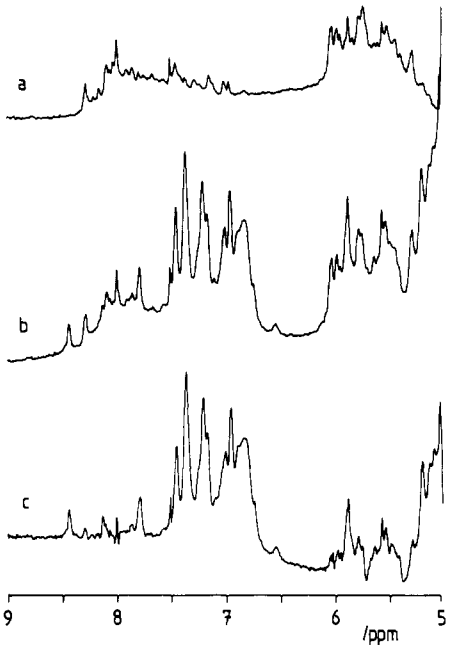

FIGURE 7: Use of the presaturation technique to examine the downfield of water spectrum of protein L25 in the 5S RNA fragment–L25 complex. (a) The spectrum of presaturated 5S RNA fragment: 0.44 mM *E. coli* MRE600 5S RNA fragment in 2 mM $MgCl_2$, 2 mM [$^2H_{11}$]Tris-^2HCl, 0.1 M KCl, and ^2H_2O, pH 7.6. (b) The spectrum of the presaturated 5S RNA fragment–L25 complex; 0.60 mM *E. coli* MRE600 5S RNA fragment–L25 complex in the same buffer. (c) Spectrum b minus spectrum a.

complex spectrum is better resolved than the comparable 5S RNA–L25 complex spectrum, as expected. Also, the reduction of the relative RNA contribution to the intensity of the aromatic region by use of a fragment for complex formation makes the protein intensity clearly visible in the complex spectrum. The difference spectrum closely resembles the spectrum in Figure 2a in the distribution of intensity, indicating that the same perturbations that occur to L25 on binding to fragment were detected upon formation of the intact 5S RNA complex. In the fragment complex spectra, the binding of L25 was seen to significantly increase the line widths of the RNA resonances.

Presaturation at 4.2 ppm in 5S RNA Fragment–L25 Complex Spectra. The presaturation experiment was also done with the L25–fragment complex. Figure 7 shows the downfield of water regions of spectra of 5S RNA fragment with presaturation at ca. 4.2 ppm (a), of the stoichiometric 5S RNA fragment–L25 complex acquired under similar conditions (b), and of the difference (c) for spectrum b minus spectrum a. In the complex spectrum aromatic region, the contributions of the bound protein moiety are clearly evident. The difference spectrum (c) is the best representation of the aromatic region of bound L25 currently available because it was acquired (i) with L25 bound to 5S RNA fragment which has only half the number of aromatic base protons of intact 5S RNA, (ii) by using a spectroscopic method which removes most of the RNA intensity before differencing, and (iii) by using a fragment which has more favorable relaxation times and therefore better spectral resolution in both free fragment and complex spectra.

Figure 5 shows spectra of free L25 (a) and of L25 bound to fragment (c). In these spectra, the effects upon the upfield-shifted methyl resonances of L25 which occur on binding to 5S RNA (in this case the 5S RNA fragment) are most clearly seen. Table I summarizes the data. Note also that the protein intensity at ca. 3.2 ppm disappears upon complex formation. Figure 3d shows the aromatic region of the Figure 5c difference spectrum for comparison with other spectra.

Table I: Chemical-Shift Differences for Protein L25 Methyl Resonances in the Free Form and in the 5S RNA–L25 Complex Spectra[a]

resonance	chemical-shift difference (ppm)		
	intact 5S–L25 complex		5S fragment–L25 complex
	H form	L form	
M1	+0.03 (3)	+0.03 (0)	+0.03 (2)
M2	−0.03 (8)	−0.03 (6)	−0.03 (0)
M3, M4	+0.02 (7)	+0.01 (9)	+0.01 (1)
M5	+0.07 (6)	+0.06 (1)	+0.06 (6)
M6, M7	+0.01 (4)	none	+0.00 (6)
1.8 ppm Met CH_3	−0.08 (8)	−0.07 (6)	−0.09 (1)
2.0 ppm Met CH_3	+0.00 (5)	+0.00 (6)	−0.00 (6)
2.1 ppm Met CH_3	−0.06 (0)	−0.05 (7)	−0.08 (3)

[a] The resonances are labeled as in Kime et al. (1981). A negative sign means a resonance moves downfield upon complex formation.

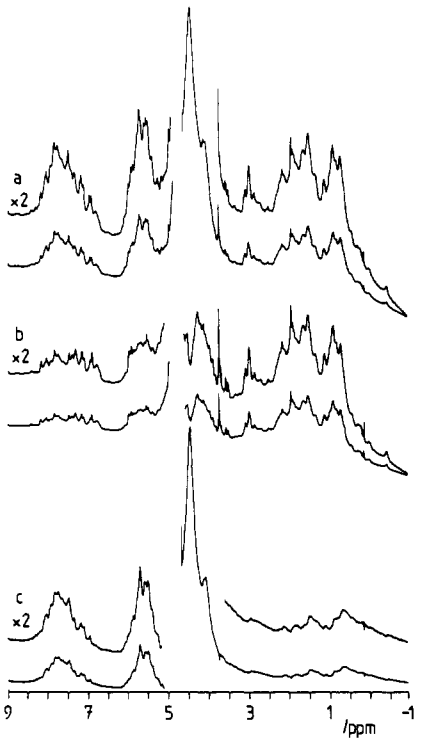

FIGURE 8: Demonstration of the effects of selective irradiation at 4.2 ppm on L-form 5S RNA–L25 complex spectra. (a) The spectrum of 0.82 mM 5S RNA–L25 complex in 20 mM K_3PO_4–^2HCl, 100 mM KCl, 0.1% [$^2H_6$]ethanol, and ^2H_2O, pH 7.5. (b) The spectrum of the same sample using the presaturation pulse sequence. (c) Spectrum a minus spectrum b.

Presaturation at 4.2 ppm in L-Form 5S RNA–L25 Complex Spectra. A presaturation experiment was done on the complex formed with L-form 5S RNA and L25. Figure 8 shows spectra of the stoichiometric L-form 5S RNA–L25 complex (a), the same sample using presaturation at ca. 4.2 ppm (b), and the difference (c) of spectrum a minus spectrum b. The protein resonances upfield of 4.0 ppm in Figure 8a indicate that the same changes in the L25 spectrum detected upon L25 binding to H-form 5S RNA (or fragment) occur when L25 binds to L-form 5S RNA.

The bound L25 aromatic region in Figure 8b is similar to that seen in the H-form 5S RNA–L25 complex (Figure 4b). Moreover, the difference spectrum in Figure 8c bears a strong resemblance to the spectrum previously published for isolated L-form 5S RNA (Kime & Moore, 1982). It appears that L25

is binding to L-form 5S RNA to form a complex in which the L25 assumes the same conformation it assumes upon forming an H-form complex and that the L-form 5S RNA retains its L-form character in the nucleoprotein complex; i.e., L25 does not appear to shift the L–H equilibrium.

Discussion

The difference spectra which provide the spectral representations of the 5S RNA moiety in the nucleoprotein complex (Figure 4c for the H form; Figure 8c for the L form) are barely distinguishable from the comparable spectra of the corresponding forms of free 5S RNA. Thus, by NMR criteria, the chemical environments of nonexchangeable protons in the RNA can be only modestly perturbed by complex formation. This supports the conclusion from NMR studies of the downfield region of the spectrum of the 5S RNA–L25 complex performed in ^1H_2O (Kime & Moore, 1983a) that the structural changes the RNA suffers upon binding L25 are small.

The spectral representations of the protein L25 moiety in the H-form 5S RNA complex Figures 2a and 3b and Figures 3c and 5b are sufficiently similar to the representation of the L25 moiety in the 5S fragment complex (Figures 5c and 7c) (except for spectral resolution) to indicate that L25 bound to either RNA is in a similar conformation. The data for the L-form complex are less complete but suggest that L25 binds to it in much the same way that it does to the other RNAs. In the difference spectral representations of the aromatic region of bound L25, several "glitches" are seen. These are not electronic experimental artifacts but occur because the free RNA spectrum is not exactly the same as the bound RNA spectrum. Certain chemical-shift positions consistently show this effect, e.g., 7.9 and 8.2 ppm.

Comparison of the spectra of L25 in the complex with the spectra of free L25 (Figures 2, 3, and 5) shows several changes occur in the protein upon complex formation. (i) In the aromatic region, the major effect of L25 binding to RNA appears to be a redistribution of some of the intensity at ca. 6.8 ppm. Otherwise, the effects of binding are small. (ii) In the region where upfield-shifted methyl resonances occur (0.8 to −0.5 ppm), there are some slight changes in chemical shifts upon binding to RNA, but essentially the free protein pattern of resonances is retained in the complexed protein. (iii) At 3.2 ppm, a major peak in the free protein spectrum disappears upon complexation. The chemical-shift position for the resonances due to δ-CH_2 protons of isolated arginine (McDonald & Phillips, 1969) is at 3.2 ppm, and 3.3 ppm is the chemical shift of arginine δ-CH_2 proton resonances in oligopeptides (Bundi & Wuthrich, 1979) with both values obtained from samples in ^2H_2O at neutral pH. It is not unreasonable that the arginine side chains in free globular L25 should have properties like those they have in the isolated amino acid or in oligopeptides; they are predominantly surface residues. Thus, their δ-CH_2 resonances should occur near 3.2 ppm in free L25. The loss of intensity at 3.2 ppm suggests that arginine side-chain protons undergo an alteration in chemical environment or relaxation properties upon complexation.

There are six arginine residues in L25 at positions 9, 18, 19, 21, 79, and 93 (Dovgas et al., 1975; Bitar & Wittmann-Liebold, 1975; Alakhov et al., 1976). This distinctive perturbation of arginine intensity at 3.2 ppm (and the perturbations seen in the 1.7, 1.8, and 1.9 ppm positions may also be related to arginine side-chain effects) could indicate that arginine side chains play a significant role in the protein–nucleic acid interaction. By the same logic, the absence of detectable perturbations to the lysine intensity at ca. 3.0 ppm may indicate that lysines are unimportant in the complex formation.

The modest changes in the aromatic region of L25 which occur upon complex formation, the confirmation that the aromatic ring-current-shifting centers in the protein, which give rise to upfield ring-current-shifted methyls, do not move relative to the upfield-shifted methyl groups (because the methyl chemical-shift pattern changes little), and the very small effects in the RNA spectra which occur upon complex formation all indicate that intercalation of protein aromatic side chains into base-stacked RNA helices or of RNA bases into a stacked array of protein aromatic side chains does not play an important role in the mechanism of protein L25 binding to 5S RNA. The best known example of an intercalation mechanism for nucleoprotein binding is the gene 5 protein–single-stranded DNA system [see O'Connor & Coleman (1983) and references cited therein]. In that case, intercalation is signaled in the NMR spectrum by substantial upfield shifts of both protein and DNA aromatic resonances. This type of spectral phenomenon is not seen here.

The limited nature of the chemical shift perturbations seen in the L25 spectrum upon RNA binding suggests that the protein's structure is not grossly altered in the process. It would appear, therefore, that a TMV-like mechanism (Bloomer et al., 1978; Stubbs et al., 1976) for RNA binding is not operative in the L25 case either. There is no evidence for the induction of new structure in the protein upon complex formation. In drawing this conclusion, one must bear in mind that NMR spectroscopy of the kind demonstrated above has limitations with respect to assessing conformational changes. For example, were L25 to consist of two domains whose relationship changes upon RNA binding but whose internal structures were preserved, very little might be seen by way of spectral changes. On the other hand, relatively small changes in the relationship of aliphatic and aromatic side chains within a domain should have drastic effects on the spectrum. Indeed, it is the absence of these kinds of ring-current effects which enables one to conclude in this case that the internal structure of L25's domain(s) does not change much upon RNA binding and to conclude that intercalation is not operative in this binding interaction. Moreover, one would expect that the induction of secondary and tertiary structure in previously random-coil regions of a protein due to nucleic acid binding, as characterized by TMV protein, would likewise be readily detected.

Acknowledgments

We thank Darcy Fazio and Betty Freeborn for their able technical assistance. Gregory Dalach and Elizabeth Roche contributed to the development of the work. We thank Suzan Vrba for her assistance with the preparation of the manuscript.

Registry No. Arginine, 74-79-3.

References

Alakhov, Y. B., Vinokurov, L. M., Dovgas, N. V., Markova, L. F., Mednikova, T. A., Motuz, L. P., Kashparov, I. A., & Ovchinnikov, Yu. A. (1976) *Bioorg. Khim. 2*, 5–18.

Bitar, K. G., & Wittmann-Liebold, B. (1975) *Hoppe-Seyler's Z. Physiol. Chem. 356*, 1343–1352.

Bloomer, A. C., Champness, J. N., Bricogne, G., Staden, R., & Klug, A. (1978) *Nature (London) 276*, 362–368.

Bundi, A., & Wuthrich, K. (1979) *Biopolymers 18*, 285–297.

Campbell, I. D., & Dobson, C. M. (1979) *Methods Biochem. Anal. 25*, 1–133.

Campbell, I. D., Dobson, C. M., Jeminet, G., & Williams, R. J. P. (1974) *FEBS Lett. 49*, 115–119.
Douthwaite, S., Garrett, R. A., Wagner, R., & Feunteun, J. (1979) *Nucleic Acids Res. 6*, 2453–2470.
Dovgas, N. V., Markova, L. F., Mednikova, T. V., Vinokurov, L. M., Alakhov, Yu. B., & Ovchinnikov, Yu. A. (1975) *FEBS Lett. 53*, 351–354.
Johnston, P. D., & Redfield, A. G. (1978) *Nucleic Acids Res. 5*, 3913–3927.
Kime, M. J., & Moore, P. B. (1982) *Nucleic Acids Res. 10*, 4973–4983.
Kime, M. J., & Moore, P. B. (1983a) *Biochemistry 22*, 2622–2629.
Kime, M. J., & Moore, P. B. (1983b) *FEBS Lett. 153*, 199–203.
Kime, M. J., & Moore, P. B. (1983c) *Biochemistry 22*, 2615–2622.
Kime, M. J., Ratcliffe, R. G., Moore, P. B., & Williams, R. J. P. (1981) *Eur. J. Biochem. 116*, 269–276.
McDonald, C. C., & Phillips, W. D. (1969) *J. Am. Chem. Soc. 91*, 1513–1521.
O'Connor, T. P., & Coleman, J. E. (1983) *Biochemistry 22*, 3375–3381.
Stubbs, G. J., Warren, S. G., & Holmes, K. C. (1976) *Nature (London) 267*, 216–221.

Nature of Steady-State and Newly Synthesized Mitochondrial Messenger Ribonucleic Acids in Mouse Liver and Ehrlich Ascites Tumor Cells†

Kolari S. Bhat, Gouder R. Kantharaj,‡ and Narayan G. Avadhani*

ABSTRACT: The steady-state mitochondrial mRNAs in Ehrlich ascites tumor cells and mouse liver were identified by the Northern blot analysis using nick-translated mtDNA and ^{32}P-labeled cDNA probes. The steady-state mRNA species were compared with the poly(A)-containing RNA synthesized in vitro in isolated mitoplasts. The results show that the isolated mitoplast system can efficiently transcribe almost all of the poly(A)-containing RNAs detected in the steady-state RNA population. It is also seen that the mode of transcription and maturation of mitochondrial mRNAs in different mouse tissues are identical. The results of Northern blot analyses suggest that there may be at least two different modes of mRNA maturation depending upon if the reading frames are interrupted by tRNA cistrons or not. mRNAs for reading frames with adjacent tRNA cistrons downstream appear to be processed from very short-lived precursors. In contrast, mRNAs coded by adjacently located reading frames with no interrupting tRNA genes such as URF3–cyt ox III and URF5–cyt *b* are processed from relatively long-lived precursors. The in vitro pulse-labeling studies also show that almost all of the poly(A)-containing mRNAs are transcribed at nearly identical rates, suggesting that the major regulation of mt gene expression may occur at the level of translation or mRNA decay. The present experiments have also identified a 1.85-kb poly(A)-containing RNA as the putative URF5 mRNA.

Mitochondria from different mammalian cells contain a circular genome of about 16-kb[1] DNA (Borst, 1972; Dawid et al., 1976). Recent DNA sequence analyses have shown that mt genomes from human (Anderson et al., 1981), mouse (Bibb et al., 1981), and bovine (Anderson et al., 1982) cells contain information for coding 2 rRNAs, 22 tRNAs, and 13 potential mRNAs. Of the 13 mRNA reading frames, 5 have been identified as genes coding for 3 mitochondrially synthesized subunits of cytochrome *c* oxidase, designated as cyt ox I, cyt ox II, and cyt ox III, subunit 6 of ATPase, and the 42-kdalton cyt *b* protein (Anderson et al., 1981, 1982; Bibb et al., 1981). The products of the remaining eight reading frames designated as URFs have not yet been identified. By use of partial nucleotide sequencing and physical mapping methods, putative mRNAs coded by 12 different reading frames located on the H strand of the mt genome have been identified in both human (Gelfand & Attardi, 1981; Montoya et al., 1981; Ojala et al., 1981) and mouse (Battey & Clayton, 1978; Van Etten et al., 1982) systems. The precise mode of transcription and the maturation pathway for a number of mRNAs coded by the mt genome in mammalian cells, however, remain to be elucidated. Similarly, it is unknown if the mt genome is expressed uniformly irrespective of tissue types or if there are differential rates of transcription and turnover of mRNAs in different tissues.

Recent studies in our laboratory showed that digitonin-treated mitoplasts can actively synthesize proteins resembling in vivo mt translation products (Bhat et al., 1981, 1982) and also accurately transcribe and process mt-specific rRNA in vitro (Kantharaj et al., 1983). In the present paper, we have used this in vitro mitoplast system to study the mode of synthesis of poly(A)-containing RNAs, putative mt mRNAs, and compared them with the steady-state mt mRNAs from mouse liver and Ehrlich ascites tumor cells. Our results show that the in vitro mitoplast system can synthesize almost all of the

† From the Laboratories of Biochemistry, Department of Animal Biology, School of Veterinary Medicine, University of Pennsylvania, Philadelphia, Pennsylvania 19104. *Received May 23, 1983.* This investigation was supported in part by grants from the National Science Foundation (PCM 80-22646) and the National Institutes of Health (GM 29037).

‡ Permanent address: Department of Botany, The National College, Bangalore, India.

[1] Abbreviations: kb, kilobase, kbp, kilobase pair; mt, mitochondria; mtDNA, mitochondrial DNA; rRNA, ribosomal RNA; mRNA, messenger RNA; tRNA, transfer RNA; poly(A), poly(adenylic acid); poly(U), poly(uridylic acid); EDTA, disodium ethylenediaminetetraacetate; $NaDodSO_4$, sodium dodecyl sulfate; Hepes, *N*-(2-hydroxyethyl)-piperazine-*N'*-2-ethanesulfonic acid; URF, unidentified reading frame; H strand, heavy strand; L strand, light strand; cyt ox (CO in Figure 1), cytochrome oxidase; cyt *b*, cytochrome *b*; dT, thymidine; Tris, tris(hydroxymethyl)aminomethane.

0006-2960/84/0423-1695$01.50/0